Monthly Notices
of the
ROYAL ASTRONOMICAL SOCIETY

MNRAS **456,** 3168–3174 (2016) doi:10.1093/mnras/stv2879

Simultaneous optical monitoring of BL Lacertae object S5 0716+714 with high temporal resolution

Zhongyi Man,[1,2,3] Xiaoyuan Zhang,[1] Jianghua Wu[1]★ and Qirong Yuan[4]

[1]*Department of Astronomy, Beijing Normal University, Beijing 100875, China*
[2]*Department of Astronomy, Physics School, Peking University, Beijing 100871, China*
[3]*Kavli Institute for Astronomy and Astrophysics (KIAA), Peking University, Beijing 100871, China*
[4]*Department of Physics and Institute of Theoretical Physics, Nanjing Normal University, Nanjing 210046, China*

Accepted 2015 December 7. Received 2015 December 4; in original form 2015 August 4

ABSTRACT

We have monitored the BL Lacertae object S5 0716+714 simultaneously in the *B*, *R* and *I* bands on three nights in 2014 November. The average time resolution is quite high (73, 34 and 58 s for the filters *B*, *R* and *I*), which can help us trace the profile of the variation and search for the short inter-band time delay. Intra-day variability was about 0.1 mag on the first two nights and more than 0.3 mag on the third. A bluer-when-brighter colour behaviour was found. A clear loop path can be seen on the colour–magnitude diagram of the third night, revealing possible time delays between variations at high and low energies. It is the first time that the intra-day spectral hysteresis loop has been found so obviously in the optical band. We used the interpolated cross-correlation function method to further confirm the time delay and calculated the values of lag between light curves at different wavelengths on each night. On the third night, variations in the *R* and *B* bands are approximately 1.5 min lagging behind the *I* band. Such optical time delay is probably due to the interplay of different processes of electrons in the jet of the blazar.

Key words: galaxies: active – BL Lacertae objects: individual: (S5 0716+714) – galaxies: photometry.

1 INTRODUCTION

As the most extreme class of active galactic nuclei, blazars exhibit rapid and large amplitude variability from radio to gamma-ray bands (e.g. Raiteri et al. 2003; Villata et al. 2008; Bonning et al. 2012; Sandrinelli, Covino & Treves 2014), high and variable polarization (e.g. Sasada et al. 2008; Gaur et al. 2014) and a non-thermal continuum. In general, a blazar is believed to be powered by a central black hole with its accretion disc producing and accelerating relativistic jets outwards. This may explain its extreme behaviour considering the jet is oriented very close to the line of sight (Urry & Padovani 1995). A typical spectral energy distribution (SED) of BL Lacs is constituted of two components, according to the peak frequency of the low-energy component, we can classify BL Lacs as low-/intermediate-/high-frequency-peaked BL Lac objects (hereafter, LBL/IBL/HBL).

S5 0716+714 is one of the best-studied BL Lac objects. Its redshift was estimated as $z = 0.31 \pm 0.08$ by Nilsson et al. (2008) with the photometric detection of the host galaxy. More recently, a limit of $0.2315 < z < 0.322$ was given by Danforth et al. (2013). Multiwavelengths campaigns have been devoted to study the SED of the source (e.g. Ferrero et al. 2006; Giommi et al. 2008; Villata et al. 2008). Because its peak frequency of the low-energy component of SED lies between 10^{14} and 10^{15} Hz, the object was classified as an IBL (Giommi et al. 2008).

Among all the most extremely variable blazars, BL Lac S5 0714+716 is one with confirmed and documented variability at all wavelengths and on different time-scales ranging from minutes to decades. Rani et al. (2013) investigated radio to gamma-ray variability of the source from 2007 to 2011, and found correlation between radio and gamma-ray variations. Liu et al. (2012) found its intra-day variability (IDV) and long-term flux variations at 4.8 GHz. It is widely confirmed that the source performs almost continuous microvariability activity with a duty circle close to 1club (e.g. Wagner et al. 1996; Wu et al. 2007, 2012; Webb, Bhatta & Hollingsworth 2010; Chandra et al. 2011; Zhang et al. 2012; Hu et al. 2014). In order to trace such very fast variations, high time resolution is required for the monitoring campaigns. For example, Bhatta et al. (2013) conducted a 72 h Whole Earth Blazar Telescope microvariability observation with exposure time from 30–150 s. The exposure time for Hu et al. (2014) is 15–300 s, and the time for Dai et al. (2013) is 30–480 s.

Attempts have been made to detect time delays in different frequency of S5 0716+714: time lags among radio, optical, X-ray and gamma-ray bands have been calculated (e.g. Rani et al. 2013; Liao

★ E-mail: jhwu@bnu.edu.cn

et al. 2014) as several days. For optical bands, a possible lag of about 11 min was found by Poon, Fan & Fu (2009) between the *B* and *I* bands. Zhang (2010) claimed lags of a few minutes between different optical bands. Wu et al. (2012) found variations in the *B* and *V* bands lead that of the *R* band by about 30 min on one night. However, the time delays are sometimes too short to be detected. Gupta et al. (2012) tried to calculate the time delay between *V* and *R* bands, but the z-transformed discrete correlation function (ZDCF) peak is too close to zero and the exposure time of their observation is 180 s which may be longer than the lag itself. The high temporal resolution of our observation can help us obtain more convincing optical time delay of S5 0716+714.

The mechanism leading to blazar variability remains unsettled. One of the most favoured scenarios is the shock-in-jet model: shock arises from the root of the jet and propagates outwards, accelerating electrons and compressing magnetic fields (Marscher & Gear 1985; Qian et al. 1991). However, other scenarios like microlensing effects (Nottale 1986), geometric effects (Camenzind & Krockenberger 1992) and interstellar scintillation (Rickett et al. 2001; Liu et al. 2012), etc. also contribute in variability. Hu et al. (2014) ascribed the IDV of S5 0716+714 to the intrinsic shock-in-jet models and geometric effects. Zhang et al. (2012) argued that the turbulent process leads to variability. In fact, the mechanism of variability seems complicated than just one simple explanation.

In order to trace the intra-day optical variability of S5 0716+714 in multiple colour and search for the possible time delays, we carried out short term observations in the *B*, *R* and *I* broad-bands with three telescopes on the nights of 2014 November 1, 2 and 3. Our temporal resolution are 73 s, 34 and 58 s for three days average of the *B*, *R* and *I* bands, which are higher than some of other campaigns. Hence, we can obtain a more detailed record of the microvariability and search for possible optical inter-band time delay. The observation, data reduction, and results are presented and discussed in the following sections.

2 OBSERVATIONS AND DATA REDUCTION

We performed a three-day observation of S5 0716+714 with three telescopes at the Xinglong Station of the National Astronomical Observatories of China (NAOC). The detail of the telescopes is shown in Table 1. Observations started from the mid-nights of 2014 November 1, 2 and 3 simultaneously on three telescopes, ended on the next morning before 7 am, the average time span of each night are 4.50 h, 5.26 and 5.10 h, respectively. The exposure time were set as 70, 10 and 40 s for the filters *B*, *R* and *I*, respectively, which were adjusted referring to the seeing, moon phase, weather conditions then, but never exceed 80 s. The average exposure time for each band were 62.5, 16.3 and 36.4 s and the average temporal resolution were 73, 34 and 58 s. We used the IRAF[1] to conduct the data reduction procedure. Four stars (2, 3, 5, 6 in Fig. 1) were selected as comparison stars. The standard magnitudes of the stars in the *B*, *R* and *I* bands are given by Villata et al. (1998) and Ghisellini et al. (1997) (listed in Table 2). The magnitude of S5 0716+714 was measured relative to the four comparison stars. The aperture radii, inner radius of the sky annuli, the width of the sky annuli are set according to the full width at half-maximum derived from the images.

The photometric errors of our observations are all below 0.07 mag, most of which are around 0.01 mag. The distribution of photometric error is shown in Fig. 2. The proportion of error over 0.02 mag is only 0.0026 representing 9 data points in *R* band on the end of the second night. Their relatively large photometric errors were the result of the sky background getting brighter at the beginning of morning twilight. We obtained the total number of the data points as 3444: 718 images for the *B* band, 1717 for the *R* band, and 1009 for the *I* band.

Table 1. Parameters of the telescopes.

Telescopes[a]	Filter	CCD resolution	CCD view
60 cm reflecting telescope	*R*	1.06 arcsec pixel^{-1}	11 arcmin × 11 arcmin
80 cm Cassegrain reflector	*I*	0.51 arcsec pixel^{-1}	18 arcmin × 18 arcmin
85 cm Cassegrain reflector	*B*	1 arcsec pixel^{-1}	33 arcmin × 33 arcmin

[a] All three telescopes are located at the Xinglong Station of the National Astronomical Observatories of China (NAOC).

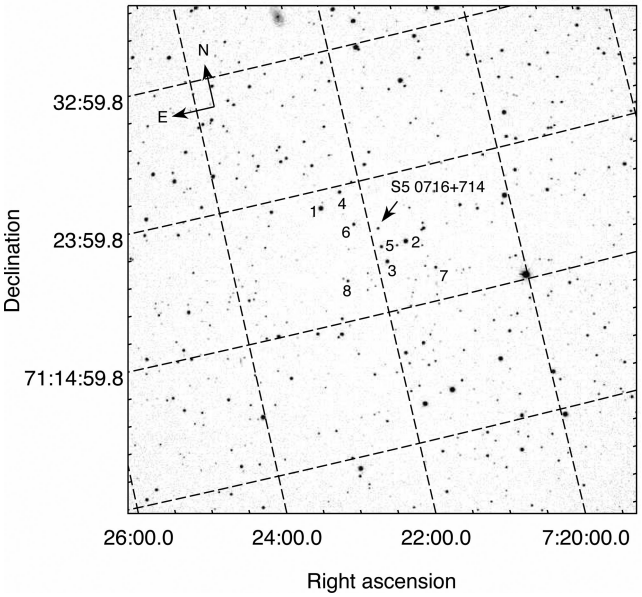

Figure 1. Finding chart of S5 0716+714 on the *I* band on the third night. The comparison stars are adopted from Villata et al. (1998).

Table 2. The standard magnitudes of the four reference stars.

Reference stars[a]	*B*	*R*	*I*
2	12.02	11.12	10.92
3	13.04	12.06	11.79
5	14.15	13.18	12.85
6	14.24	13.26	12.97

Note. [a] Standard magnitudes are given by Villata et al. (1998) and Ghisellini et al. (1997).

[1] IRAF is distributed by the National Optical Astronomy Observatories, which are operated by the Association of Universities for Research in Astronomy, Inc., under cooperative agreement with the National Science Foundation. (http://iraf.noao.edu).

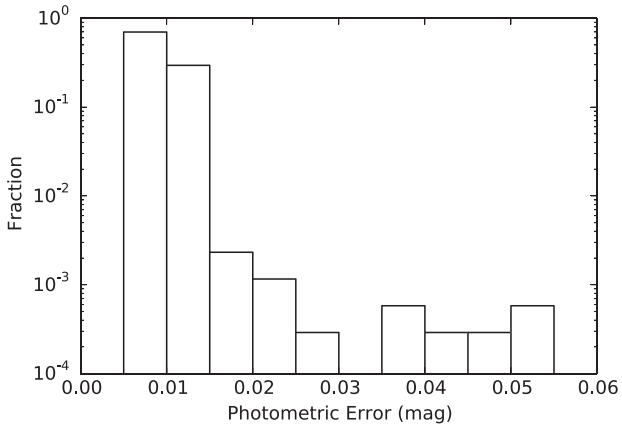

Figure 2. The distribution of photometry error of all observations.

3 LIGHT CURVES

3.1 Variability test

In order to verify the IDV of S5 0716+714, we performed two robust statistic methods introduced by de Diego (2010): one-way analysis of variance (ANOVA) test and χ^2 test. In one-way ANOVA test, we sampled observation data every 30 min, so the total number of groups $k \sim 11$ in each band every night. In χ^2 test, we considered a correction factor $\eta = 1.5$ (Stalin et al. 2004; Gupta et al. 2008), and we assumed the rescaled error $\sigma_{\rm real} = \eta\sigma$ as real error in test calculation.

The results of both tests are presented in Table 3. All 9 F values of one-way ANOVA test are significantly larger than critical values of $\alpha = 0.001$. However, 2 of 9 χ^2 values are slightly smaller than critical values of $\alpha = 0.001$, which were noted as V^* in the column of result. Those with both F value and χ^2 value over critical values were noted as V (variable). This incompatibility can be ascribed to the discrepancy of power in these methods and was discussed by de Diego (2010). As a result, we can conclude that IDV can be found on all three nights in all three bands.

3.2 Intra-day variability

The overall light curves in the B, R and I bands are presented in Fig. 3. Magnitudes of the B and I bands are shifted closer to one another in order to provide a better view. On the first night, the time interval between the maximum and the minimum of the variation is about 2.6 h in the I band, during which the brightness varied by 0.08 mag. The pattern of the curve seems approximately a sinusoidal curve, such a curve of this source was also found by Wu et al. (2005). On the second night, two small flares can be seen in the light curves in the R and B bands, but it seems there is an extra flare before the two flares in the I band. The cause of such difference is unclear, but at least it should not be attributed to our data reduction. Microlensing effect and interstellar scintillation should be excluded since the former influences emission in all wavelengths (Wagner & Witzel 1995) while the latter would not affect the optical variation.

Light curves on the third night reveals violent variability in all three bands compared with earlier days (see Fig. 3). A double-peak structure can be seen clearly with five small sub-peaks overlapped on. At first, the object turned bright dramatically to the first peak, then it came down a little before reaching another peak again. The second peak is brighter than the first, and it is only 1.3 h between the two peaks. The brightness turned down quickly followed by a small flare at the end of the observation. By visual inspection, we can see quasi-periodic oscillations (QPO) e.g. three flares on the second peak separated by about 20 min.

To expose these peaks more precisely, we filtered the original light curve with a finite impulse response (FIR) filter. The length of filter and cut-off frequency were set to be 20 and 0.1 min^{-1}, separately. The consequence was shown in lower panel of Fig. 4. Five flares were marked by vertical dashed lines. The time intervals between each flare are 10.14, 25.47, 17.62 and 17.62 min, respectively. Despite the second flare shifted to an earlier time, the separation between first and last flare is ∼71 min, which is almost four times of the last two intervals. This 17.6 min period is close to ∼25 min (Gupta, Srivastava & Wiita 2009) and ∼15 min (Rani et al. 2010) in the historical observation of QPO of this source.

Specifically, the IDV of the third day is remarkable for its large amplitude and fast change rate which exceeds many of its historical records. In literature, S5 0716+714 was observed to vary by 0.117 mag in 1.1 h in c band (Dai et al. 2013). Nesci, Massaro & Montagni (2002) found a maximum rising rate of 0.16 mag h^{-1}. The fastest changing rate of almost 0.38 mag h^{-1} was detected by Chandra et al. (2011). Our observation reveals a maximum changing rate of 0.347 mag h^{-1} (B band) which has been quite a high rate so far. In other blazars, the change rate of variation could be even higher i.e. PKS 2155-304 was detected to have a very fast variability rate of 0.43 mag h^{-1} (Sandrinelli et al. 2014).

In general, the trends of light curves in different bands are basically the same but with different amplitude. On the first two days, amplitudes of light curves in the B and R bands are slightly larger than that of the I band. The amplitude of magnitude on the third day decreases with wavelengths: the rising amplitude is 0.27 mag for B band but 0.25 mag for I band. This trend has been confirmed by a

Table 3. Results of one-way ANOVA test and χ^2 test of light curves in each band for each day.

			One-way ANOVA		χ^2 test		
JD	Band	N	F_{ν_1,ν_2}	$F^{0.001}_{\nu_1,\nu_2}$	χ^2	$\chi^2_{0.001,\nu}$	Result
245 6963	B	198	91.6143	3.0172	233.6034	264.0754	V^*
245 6963	R	797	182.3321	3.1388	870.5844	925.0195	V^*
245 6963	I	259	378.7852	3.0904	776.8546	333.9289	V
245 6964	B	234	148.3069	2.9881	426.4335	305.4426	V
245 6964	R	434	142.3280	3.0352	720.6714	529.6648	V
245 6964	I	275	90.9400	3.0822	628.1363	352.0720	V
245 6965	B	233	321.4710	3.2459	7455.161	304.2994	V
245 6965	R	491	401.1203	3.0261	8631.511	592.4640	V
245 6965	I	475	360.2808	3.0285	11 665.65	574.8719	V

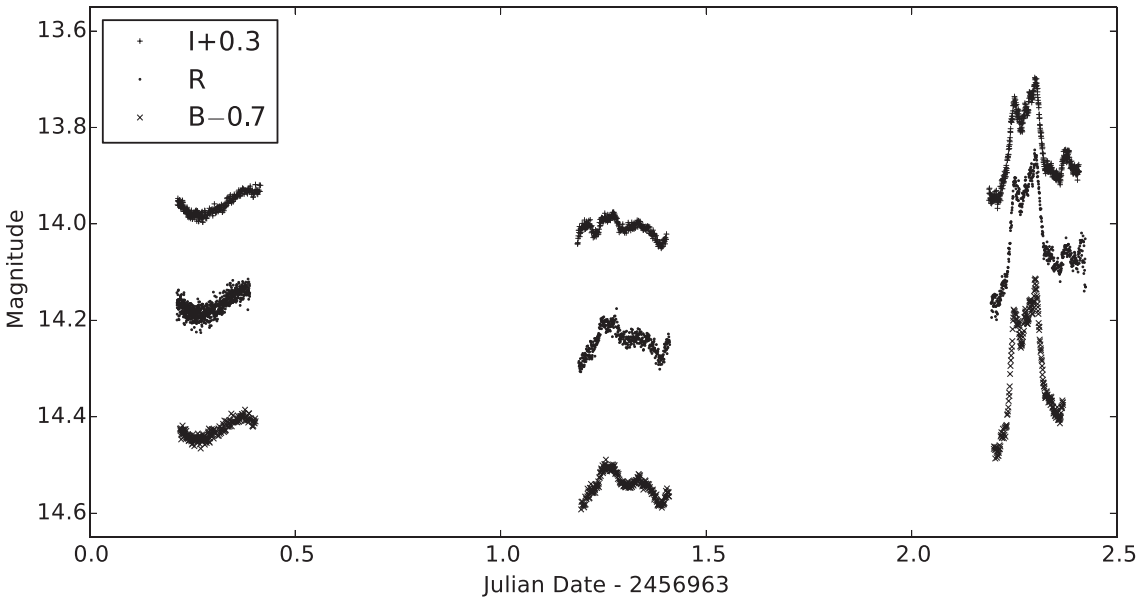

Figure 3. Overall light curves of S5 0716+714.

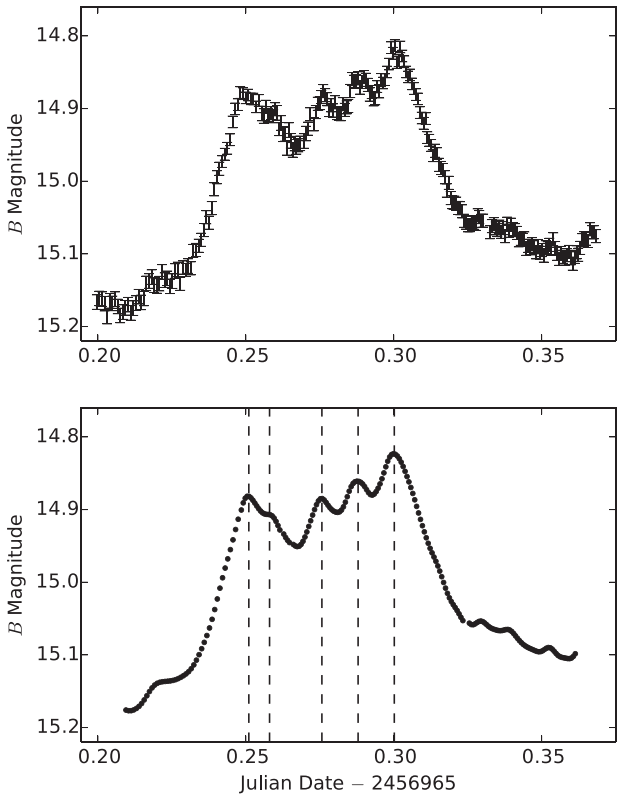

Figure 4. Upper panel: light curve of S5 0716+714 on the third night in B band. A maximum changing rate of 0.347 mag h^{-1} (B band) was detected. Lower panel: light curve after smoothed by FIR filter, five flares are marked by vertical dashed lines, and demonstrate QPOs.

number of authors for different blazars (e.g. Gupta et al. 2012; Wu et al. 2012; Dai et al. 2013; Man et al. 2014). The trend, however, may lead to the special colour behaviour as discussed in the next section.

4 COLOUR BEHAVIOUR AND SPECTRAL HYSTERESIS

We investigated the colour–magnitude relationship for each separate night. Specifically, we use $B - R$, $R - I$ and $B - I$ to represent the colour of the target, trying to show how they are related to B, R and I magnitudes, respectively. The results displayed in Fig. 5 reveal that the colour of the object remained almost unchanged during the first night, which may explain the sinusoidal curve on this night: this has been reported occasionally before (e.g. Wu et al. 2005; Poon et al. 2009). Such achromatic variation is probably caused by the lighthouse effect as a geometric factor in shock-in-jet model according to Camenzind & Krockenberger (1992): when enhanced particles are moving relativistically towards an observer on helical trajectories in the jet, flares will be produced by the sweeping beam whose direction varies with time. On the second night, a slight bluer-when-brighter (BWB) chromatism can be seen; on the third night, however, the object exhibited strong BWB chromatism. Such BWB trend is common for many blazars, especially for BL Lacs. S5 0716+714 has shown strong BWB in both intra-night and inter-night time-scales in literature (Raiteri et al. 2003; Wu et al. 2007; Chandra et al. 2011; Dai et al. 2013; Hu et al. 2014). The mechanism of BWB was simulated and attributed to the difference of the amplitudes and cadences at different wavelengths (Dai et al. 2011). For flat spectrum radio quasar, both BWB and redder-when-brighter trend can be found, and it is hard to conclude which dominates (Gu et al. 2006; Hu et al. 2006; Gu & Ai 2011).

In Fig. 5, a loop-like pattern can be seen on the third day's colour–magnitude diagrams of $B - I$ versus I and $R - I$ versus I. By examining the order of the points, we found the loop in the third day's colour–magnitude diagram traced anti-clockwise. It is the first time that the intra-day spectral hysteresis loop has been found so obviously in the optical band. Such loop is not a general feature of colour evolution. Bonning et al. (2012) claimed OJ 287 move around on the circular locus in colour–magnitude space. Dai et al. (2013) found an anti-clockwise loop in intra-day colour behaviour of S5 0716+714. Xilouris et al. (2006) have reported the similar pattern in optical band. In other regime like gamma-ray and X-ray, the loop path has been reported frequently (e.g. Sembay et al. 1993;

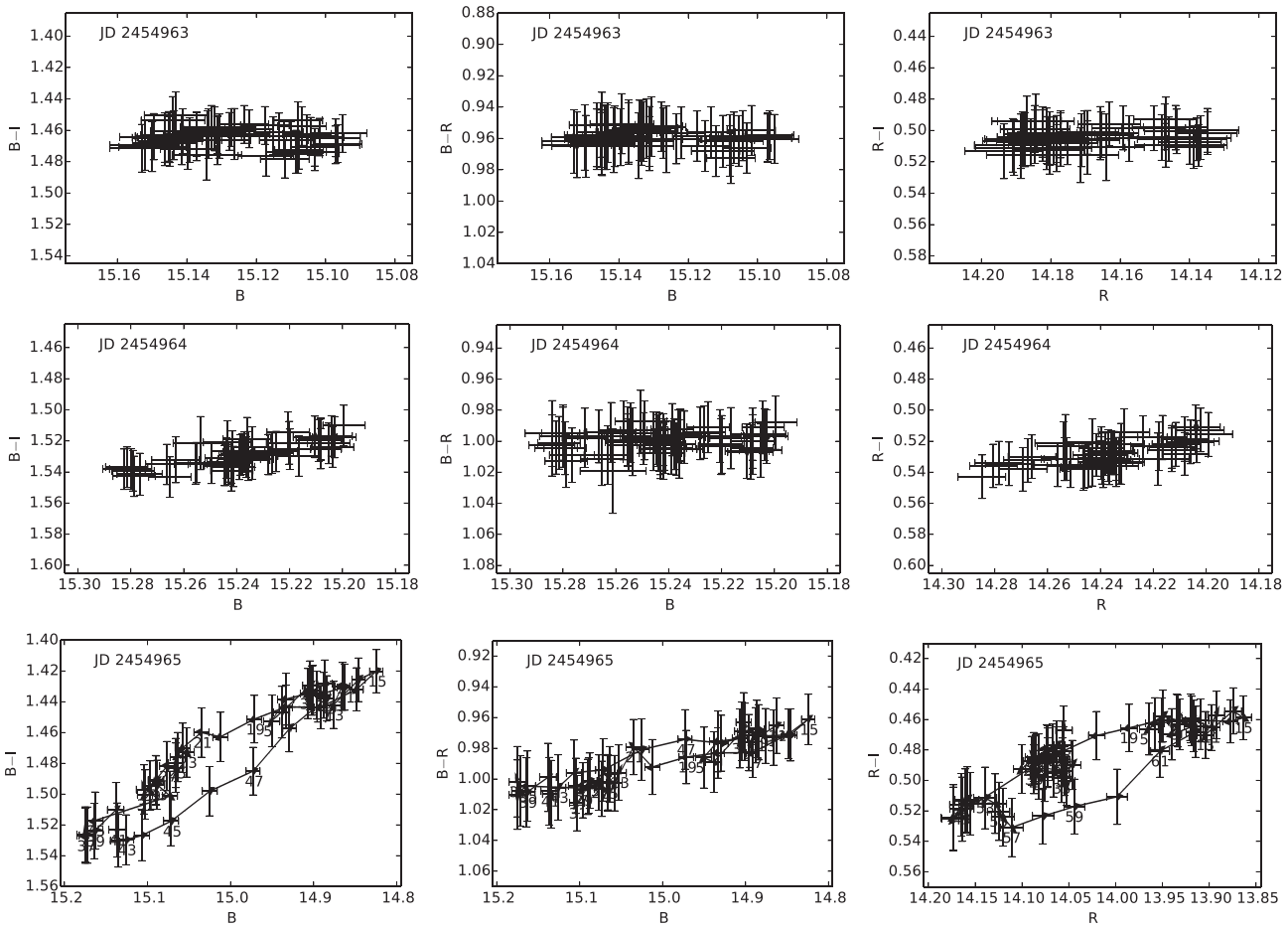

Figure 5. Colour behaviour of S5 0716+714 on three nights. Top three diagrams demonstrate the absence of colour variation on the first night; three in the middle reveal BWB on the second night; colour evolution on the third night is presented on the bottom three diagrams as clear loop paths, arrows are plotted to show the direction of the loop.

Takahashi et al. 1996; Zhang et al. 1999; Malizia et al. 2000; Zhang et al. 2002; Albani et al. 2007; Kataoka et al. 2010).

5 CROSS-CORRELATION ANALYSIS AND TIME LAGS

We performed a cross-correlation analysis to search for the possible lag between variations in different bands. There are some cross-correlation methods like the discrete correlation function method (Camenzind & Krockenberger 1992) and the ZDCF method (Alexander & Netzer 1997). Here we use the interpolated cross-correlation function (ICCF) method to estimate the lags and their errors (Gaskell & Peterson 1987). This is a flux-randomization approach, the model-independent Monte Carlo realization was used to estimate the error, and each realization is based on a randomly chosen subset of the original data points, namely the random subset selection. Considering the intervals between our observations are small, the low-order interpolation in ICCF can do a reasonable approximation to the true behaviour of the light curve (Peterson et al. 1998, 2004).

In our work, 5000 independent Monte Carlo realizations were performed on the light curves of each day. The results are listed in the Table 4. As can be seen in the table, lags of the first two days are with large relative error (greater than 1), so the results are not quite reliable. However, on the third night, especially for the *B* and *I*, *R* and *I*, the relative errors become less than 50 per cent, which suggests variations in the *R* and *B* bands are lagging behind that of *I* band by (1.308 ± 0.603) and (1.445 ± 0.511) min, respectively. Noting that the temporal resolution of our observation is shorter than the lag, and the order of variations in different bands is the same as suggested by its spectral evolution in previous chapter, the time lags given by ICCF between the *B* and *I*, *R* and *I* bands are thereby relatively convincing on the third night.

Table 4. Time lags given by ICCF method (Unit: minutes).

Date	*B*−*R*	*R*−*I*	*B*−*I*
November 1st	− 3.538 ± 5.973	− 5.703 ± 6.988	− 9.165 ± 8.271
November 2nd	0.997 ± 1.911	− 0.429 ± 3.002	− 0.313 ± 2.943
November 3rd	0.336 ± 0.500	1.308 ± 0.603	1.445 ± 0.511

So far, there has not been an exactly justifiable theoretical interpretation of such spectral hysteresis. Among many attempts the one given by Kirk & Mastichiadis (1999) is mostly favoured: in the blazar emission models like the synchrotron self-Compton model (Mastichiadis & Kirk 1997), spectral shape is influenced by particle acceleration ($\tau_{\rm acc}$), synchrotron cooling ($\tau_{\rm syn}$) and intrinsic variability ($\tau_{\rm var}$, which determines the flare duration $t_{\rm flare}$; Kirk, Rieger & Mastichiadis 1998; Kirk & Mastichiadis 1999; Cui 2004;

Sato et al. 2008). The interaction among different processes will possibly lead to spectral evolution hence a loop-like path in a colour–magnitude (or spectral-index-flux) diagram. A clockwise path may be seen when $\tau_{\rm syn} \ll \tau_{\rm var} \ll \tau_{\rm acc}$ (Kirk & Mastichiadis 1999) e.g. OJ 287 (Bonning et al. 2012) and Mkn 421 (Takahashi et al. 1996). As for anti-clockwise paths as found in our observation and PKS 2155−304(Sembay et al. 1993), the case seems to be $\tau_{\rm var} \approx \tau_{\rm syn} \approx \tau_{\rm acc}$, indicating changes propagate from low energies to high energies (Kataoka et al. 2010; Vaughan 2005). Consequently, flares in higher energies may lag behind that of the lower energies, which is in accord with both the spectral hysteresis we found and the time lags we calculated with different light curves. However, we still cannot draw any firm conclusion from a hysteresis loop on the basis of the model above. Li & Kusunose (2000) argued that the hysteresis loop is quite sensitive to various parameters in Kirk's model, such as the overall injection energy (Cui 2004).

6 CONCLUSIONS

Our monitoring session targeted the BL Lac object S5 0716+714 was performed in the *B*, *R* and *I* bands on 2014 November 1, 2 and 3 on three telescopes located at the Xinglong, China. The average temporal resolution of our observation are 73, 34 and 58 s for the *B*, *R* and *I* bands, respectively. They are set high to trace the intra-day variation of the object and to search for the optical inter-band time delays. IDV was found in each band of each day. Particularly, on November 1, we found an achromatic sine curve suggesting a possible lighthouse effect in the shock-in-jet model (Camenzind & Krockenberger 1992). On November 2, light curve in the *I* band shows an extra flare than the *B* and *R* bands. The case is rare and the cause is unclear. On November 3, we caught flares with a very fast changing rate up to 0.347 mag h^{-1} and a double-peak structure with five ∼17.6 – period QPOs overlapped on. This embodies the intense variability of the object on short time-scale.

We investigated the colour behaviour of S5 0716+714. The first night showed marginal colour variation, while the second night displayed BWB and then this trend became stronger on the third night. Particularly, loop-like paths can be seen on the $B - I$ versus I, $R - I$ versus I graphs. The loop traced anti-clockwise, possibly implying occurrence of a flare propagates from lower to higher energies, as particles are gradually accelerated into the radiating window (Kirk et al. 1998). It also suggests variations in the *B* band lagged behind that of the *I* and *R* bands. Then we use ICCF method to statistically give an estimate of the values of time delay. Time delays on the third night are (1.308 ± 0.603) min for $R - I$, (1.445 ± 0.511) min for the $B - I$. Considering the lags are longer than the temporal resolution, the results on the third day are rather plausible.

Unfortunately, we did not find any monitoring project on S5 0716+714 with high time resolution at high energies during our campaign, otherwise we could further correlate our data with data in X-ray or gamma-ray. High temporal resolution multiwavelength observation campaign may help gain a much more comprehensive understanding of radiative process and physical model of blazars.

ACKNOWLEDGEMENTS

We thank the anonymous referee for insightful comments and suggestions that helped to improve this paper. Our work has been supported by the National Basic Research Programme of China 973 Programme 2013CB834900; Chinese National Natural Science Foundation grants 11273006, 11173016, U1531242 and 11073023; and the fundamental research funds for the central universities and Beijing Normal University.

REFERENCES

Albani V. V. L., Iribarrem A. S., Ribeiro M. B., Stoeger W. R., 2007, ApJ, 657, 760
Alexander T., Netzer H., 1997, MNRAS, 284, 967
Bhatta G. et al., 2013, A&A, 558, A92
Bonning E. et al., 2012, ApJ, 756, 13
Camenzind M., Krockenberger M., 1992, A&A, 255, 59
Chandra S., Baliyan K. S., Ganesh S., Joshi U. C., 2011, ApJ, 731, 118
Cui W., 2004, ApJ, 605, 662
Dai Y., Wu J., Zhu Z.-H., Zhou X., Ma J., 2011, AJ, 141, 65
Dai Y., Wu J., Zhu Z.-H., Zhou X., Ma J., Yuan Q., Wang L., 2013, ApJS, 204, 22
Danforth C. W., Nalewajko K., France K., Keeney B. A., 2013, ApJ, 764, 57
de Diego J. A., 2010, AJ, 139, 1269
Ferrero E., Wagner S. J., Emmanoulopoulos D., Ostorero L., 2006, A&A, 457, 133
Gaskell C. M., Peterson B. M., 1987, ApJS, 65, 1
Gaur H., Gupta A. C., Wiita P. J., Uemura M., Itoh R., Sasada M., 2014, ApJ, 781, L4
Ghisellini G. et al., 1997, A&A, 327, 61
Giommi P. et al., 2008, A&A, 487, L49
Gu M. F., Ai Y. L., 2011, A&A, 534, A59
Gu M. F., Lee C.-U., Pak S., Yim H. S., Fletcher A. B., 2006, A&A, 450, 39
Gupta A. C. et al., 2008, AJ, 136, 2359
Gupta A. C., Srivastava A. K., Wiita P. J., 2009, ApJ, 690, 216
Gupta A. C. et al., 2012, MNRAS, 425, 1357
Hu S. M., Zhao G., Guo H. Y., Zhang X., Zheng Y. G., 2006, MNRAS, 371, 1243
Hu S. M., Chen X., Guo D. F., Jiang Y. G., Li K., 2014, MNRAS, 443, 2940
Kataoka J. et al., 2010, ApJ, 715, 554
Kirk J. G., Mastichiadis A., 1999, Astropart. Phys., 11, 45
Kirk J. G., Rieger F. M., Mastichiadis A., 1998, A&A, 333, 452
Li H., Kusunose M., 2000, ApJ, 536, 729
Liao N. H., Bai J. M., Liu H. T., Weng S. S., Chen L., Li F., 2014, ApJ, 783, 83
Liu X., Song H.-G., Marchili N., Liu B.-R., Liu J., Krichbaum T. P., Fuhrmann L., Zensus J. A., 2012, A&A, 543, A78
Malizia A. et al., 2000, MNRAS, 312, 123
Man Z., Zhang X., Wu J., Zhou X., Yuan Q., 2014, AJ, 148, 110
Marscher A. P., Gear W. K., 1985, ApJ, 298, 114
Mastichiadis A., Kirk J. G., 1997, A&A, 320, 19
Nesci R., Massaro E., Montagni F., 2002, PASA, 19, 143
Nilsson K., Pursimo T., Sillanpää A., Takalo L. O., Lindfors E., 2008, A&A, 487, L29
Nottale L., 1986, A&A, 157, 383
Peterson B. M., Wanders I., Horne K., Collier S., Alexander T., Kaspi S., Maoz D., 1998, PASP, 110, 660
Peterson B. M. et al., 2004, ApJ, 613, 682
Poon H., Fan J. H., Fu J. N., 2009, ApJS, 185, 511
Qian S. J., Quirrenbach A., Witzel A., Krichbaum T. P., Hummel C. A., Zensus J. A., 1991, A&A, 241, 15
Raiteri C. M. et al., 2003, A&A, 402, 151
Rani B., Gupta A. C., Joshi U. C., Ganesh S., Wiita P. J., 2010, ApJ, 719, L153
Rani B. et al., 2013, A&A, 552, A11
Rickett B. J., Witzel A., Kraus A., Krichbaum T. P., Qian S. J., 2001, ApJ, 550, L11
Sandrinelli A., Covino S., Treves A., 2014, A&A, 562, A79
Sasada M. et al., 2008, PASJ, 60, L37
Sato R., Kataoka J., Takahashi T., Madejski G. M., Rügamer S., Wagner S. J., 2008, ApJ, 680, L9

Sembay S., Warwick R. S., Urry C. M., Sokoloski J., George I. M., Makino F., Ohashi T., Tashiro M., 1993, ApJ, 404, 112
Stalin C. S., Gopal-Krishna Sagar R., Wiita P. J., 2004, MNRAS, 350, 175
Takahashi T. et al., 1996, ApJ, 470, L89
Urry C. M., Padovani P., 1995, PASP, 107, 803
Vaughan S., 2005, A&A, 431, 391
Villata M., Raiteri C. M., Lanteri L., Sobrito G., Cavallone M., 1998, A&AS, 130, 305
Villata M. et al., 2008, A&A, 481, L79
Wagner S. J., Witzel A., 1995, ARA&A, 33, 163
Wagner S. J. et al., 1996, AJ, 111, 2187
Webb J. R., Bhatta G., Hollingsworth H., 2010, American Astronomical Society Meeting Abstracts, #216, #420.11
Wu J., Peng B., Zhou X., Ma J., Jiang Z., Chen J., 2005, AJ, 129, 1818
Wu J., Zhou X., Ma J., Wu Z., Jiang Z., Chen J., 2007, AJ, 133, 1599
Wu J., Böttcher M., Zhou X., He X., Ma J., Jiang Z., 2012, AJ, 143, 108
Xilouris E. M., Papadakis I. E., Boumis P., Dapergolas A., Alikakos J., Papamastorakis J., Smith N., Goudis C. D., 2006, A&A, 448, 143
Zhang Y. H., 2010, ApJ, 713, 180
Zhang Y. H. et al., 1999, ApJ, 527, 719
Zhang Y. H. et al., 2002, ApJ, 572, 762
Zhang B. K., Dai B. Z., Wang L. P., Zhao M., Zhang L., Cao Z., 2012, MNRAS, 421, 3111

This paper has been typeset from a TEX/LATEX file prepared by the author.